Peng Guo, Wei Wan*, Lynne McCusker, Christian Baerlocher and Xiaodong Zou*

On the relationship between unit cells and channel systems in high silica zeolites with the "butterfly" projection

Abstract: Zeolites are crystalline aluminosilicate framework materials with corner sharing TO_4 (T = Al, Si) tetrahedra forming well-defined pores and channels. Many zeolites are built from similar building units (i.e., isolated units, chains or layers), which are connected in different ways to form a variety of topologies. We have identified ten zeolite frameworks that share the same two-dimensional "butterfly" net containing 5-, 6- and 10-rings: *MRE, FER, MEL, SZR, MFS, MFI, TUN, IMF, BOG and TON. Different orientations of the TO_4 tetrahedra within the layer lead to different connectivities between neighboring layers. Some layers are corrugated and some are flat, resulting in different channel systems parallel to the layer. We found some interesting relationships between the unit cell parameters and this channel system that allow the size of the channels and their directions to be deduced from the unit cell dimensions. This may facilitate the prediction of new members of this zeolite family. In addition, other zeolites containing the "butterfly" layers are also discussed.

Keywords: structure prediction; structure relationship; structure solution; zeolites.

*Corresponding authors: Wei Wan and Xiaodong Zou, Berzelii Centre EXSELENT on Porous Materials, Department of Materials and Environmental Chemistry, Stockholm University, SE-10691 Stockholm, Sweden; and Inorganic and Structural Chemistry, Department of Materials and Environmental Chemistry, Stockholm University, SE-10691 Stockholm, Sweden, E-mail: wei.wan@mmk.su.se, xzou@mmk.su.se
Peng Guo: Berzelii Centre EXSELENT on Porous Materials, Department of Materials and Environmental Chemistry, Stockholm University, SE-10691 Stockholm, Sweden; and Inorganic and Structural Chemistry, Department of Materials and Environmental Chemistry, Stockholm University, SE-10691 Stockholm, Sweden
Lynne McCusker: Inorganic and Structural Chemistry, Department of Materials and Environmental Chemistry, Stockholm University, SE-10691 Stockholm, Sweden; and Laboratory of Crystallography, ETH Zurich, CH-8093 Zurich, Switzerland
Christian Baerlocher: Laboratory of Crystallography, ETH Zurich, CH-8093 Zurich, Switzerland

Introduction

Zeolites are crystalline aluminosilicates with three-dimensional frameworks built from vertex-sharing TO_4 (T = Al, Si) tetrahedra. Each tetrahedron is connected to four other tetrahedra to form a four-connected framework with well-defined pores and channels. These channels can intersect to form one-, two- or three-dimensional channel systems. Zeolites have a broad range of applications in industry, particularly in the areas of catalysis, ion exchange and separation. It is the size of the pore openings and the dimensionality of the channel system of a given zeolite that govern the size selectivity and rate of diffusion through its channels, and therefore its suitability for a specific application.

Currently there are 225 framework types in the Database of Zeolite Structures that have been approved by the Structure Commission of the International Zeolite Association (IZA-SC) [1]. Of these, the most important framework types for catalysis are **FAU** (3D 12-ring channels) [2], **MFI** (3D 10-ring channels) [3], **MOR** (1D 8- and 12-ring channels) [4], **FER** (2D 8- and 12-ring channels) [5], and *BEA (3D 12-ring channels) [6]. Despite the low number of zeolites actually used in industrial processes, the search for new zeolites with unique channel systems continues to spark the interest of zeolite chemists. Different approaches have been developed to enumerate and predict hypothetical zeolite structures [7–10]. Indeed, millions have been predicted and are listed in databases [8, 11–13]. However, despite considerable effort, the realization of a particular structure through rational synthesis design remains a major challenge.

One strategy for predicting zeolite structures is based on combining layers found in known frameworks in different ways. For example, more than 20 framework types belong to the ABC-6 family of zeolites, which contain layers of 6-rings arranged hexagonally [14]. 4.8^2 nets are found in more than 20 zeolites [15, 16], and the tetragonal beta layer has generated a family of disordered structures known as the beta family [17–19]. The TO_4 tetrahedra in a layer can point either up or down to connect to the layer above or below to form a 3D framework. The neighboring

nets are related either by simple translations or by certain symmetry operations, and are further connected to construct different members of the same family [15]. The neighboring layers can also be rotated with respect to one another, as in the cases of the zeolite beta polymorphs [6], and the silicogermanate SU-32 (**STW**) [20]. In SU-32, the neighboring layers are rotated by 60° before being connected to form a chiral framework with helical channels.

Determining the structure of a zeolite is often challenging, because zeolites tend to have complex structures with large unit cells and often occur in the form of polycrystalline powders. Model building based on the similarities between measured unit cell dimensions and those of known structures has proven to be a powerful approach, and many zeolite structures have been solved in this way [21]. For example, the unit cell of SSZ-52 (code: **SFW**) indicated that SSZ-52 probably belonged to the ABC-6 family with a 9-layer double 6-rings (*d6r* [22]) stacking [23]. Another example is that of ITQ-38 (code: **ITG**). High-resolution electron microscopy showed that ITQ-38 had a perfect intergrowth with ITQ-22 (code: **IWW**), and two of the unit cell dimensions are similar. It was concluded that ITQ-22 and ITQ-38 were likely to contain the same layer, and a structure model for ITQ-38 could be deduced from the HRTEM image [24].

Knowing the structural relationships between different zeolite frameworks not only provides important information for structure determination, but also facilitates the prediction of new zeolite structures. Akporiaye studied the structural relationships in a series of high-silica zeolites containing 5-rings, and predicted a large number of 5-ring zeolites [25]. An important building unit is the edge-sharing 5-ring chain, which can be used to generate different 2D nets. One such net is that found for example in **MFI** (ZSM-5) [3] and **FER** (ferrierite) [5] with 5-, 6- and 10-rings (Figure 1). This net contains the well-known "butterfly" configuration of a 6-ring (the body of the butterfly) surrounded by four 5-rings (the wings) and occurs in a number of high-silica zeolite structures. For simplicity, we will refer to this net as the butterfly net hereafter, and the building layer in zeolites that corresponds to the butterfly net as the butterfly layer. The vertex symbol for this layer is $[5.6.10]_2 [5^2.10]_3 [5^2.6]$. We have identified ten zeolite frameworks from the Database of Zeolite Structures that can be built solely from this butterfly net. We call them the members of the butterfly family of zeolites. Interestingly, the channel systems in these zeolites range from one dimension (1D) to three dimensions (3D), and the pore openings vary from 8-ring to 12-ring. We noticed that the butterfly layers are significantly corrugated in some zeolites and flat in others. Corrugation of the layer would
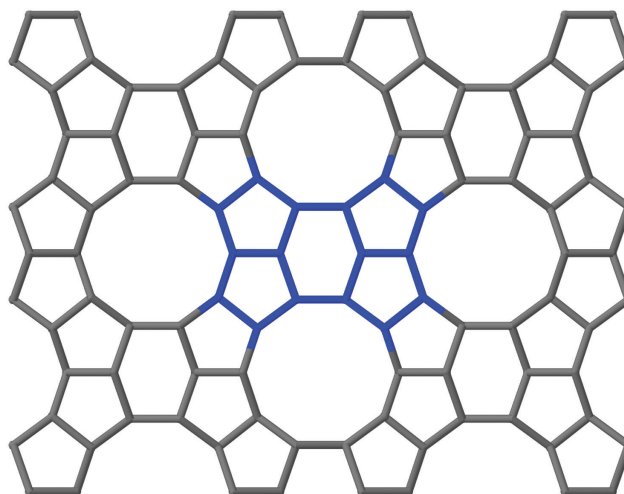

Fig. 1: A butterfly net with one "butterfly" marked in blue.

cause both the shortening of the unit cell dimensions and formation of channels parallel to the layer. Here, we study the relationship between the unit cell dimensions and channel systems in this butterfly family of zeolites.

Identification of the members of the butterfly family of zeolites

The members of the butterfly family were identified by searching the Database of Zeolite Structures [1] for the 5-1 secondary building unit (SBU), 5-, 6- and 10-rings or unit cell parameters around 20 Å and 14 Å. Search hits from each of these criteria were manually filtered and ten zeolite frameworks emerged: *MRE (ZSM-48) [26], **FER** (ferrierite) [5], **MEL** (ZSM-11) [27], **SZR** (SUZ-4) [28], **MFS** (ZSM-57) [29], **MFI** (ZSM-5) [3], **TUN** (TNU-9) [30], **IMF** (IM-5) [31], **BOG** (boggsite) [32] and **TON** (theta-1) [33]. One more framework, **MTT** (ZSM-23) [34] is closely related, but its layer is slightly different. Another nine frameworks containing the butterfly layer (**PCR** (IPC-4) [35], **–SVR** (SSZ-74) [36], **OKO** (COK-14) [37], **SFS** (SSZ-56) [38], **CON** (CIT-1) [39], **TER** (terranovaite) [40], **MEP** (melanophlogite) [41], **MTN** (ZSM-39) [42] and **GON** (GUS-1) [43]) have been identified by Topos Pro [44]. However, these frameworks cannot be built from this layer alone and will be discussed separately later in the paper.

Due to the differences in the symmetries and unit cell settings of these framework structures, the butterfly layers are oriented perpendicular to different crystallographic axes. In order to facilitate the comparison, the unit cell axes were re-configured so that the net is in the *ab*-plane

Tab. 1: Re-configured unit cell parameters (*a*, *b* and *c*), space groups and channel ring sizes for the ten members of the butterfly family of zeolites.

Framework	*a* (Å)	*b* (Å)	*c* (Å)	Δa (Å)[a]	Δb (Å)[a]	Space group	Channel ring size along *a, b, c*	Channel dimension
*MRE	14.562	20.314	8.2570	–	–	*Imcm*	–, –, 10	1D
BOG	12.669	20.014	23.580	1.893	0.300	*Ibmm*	–, 12, 10	3D
MFI	13.142	20.090	19.738	1.420	0.224	*Pbnm*	10, 10, 10	3D
MEL	13.459	20.270	20.270	1.103	0.044	$I\bar{4}m2$[b]	10, 10, 10	3D
TUN	27.845	19.597	20.015	0.640[c]	0.717	$B112/m$[d]	–, –, 10[e]	3D
TON	14.105	17.842	5.256	0.457	2.472	*Cmcm*	–, –, 10	1D
IMF	14.296	56.788	20.290	0.266	1.385[f]	*Cmcm*	10, –, 10	3D
FER	14.303	19.018	7.541	0.259	1.296	*Immm*	8, –, 10	2D
MFS	14.388	19.016	7.542	0.174	1.298	*Im2m*	8, –, 10	2D
SZR	14.401	18.870	7.5140	0.161	1.444	*Cmmm*	8, –, 10	3D

[a]The difference between the *a*- and *b*-parameters and those of *MRE (Δa and Δb). The space groups were changed to reflect the new unit cell settings, except for the tetragonal one for **MEL**.
[b]This original space group is given here. The -4 symmetry operation is along the *a*-axis in the new unit cell.
[c]This value is calculated using $a/2$.
[d]The unique axis is the *c*-axis and $\gamma = 93.2°$. The full H-M symbol is given here for clarity.
[e]The 10-ring channels are along the $[1\bar{1}0]$ direction.
[f]This value is calculated using $b/3$.

with $a \approx 14$ Å and $b \approx 20$ Å. The same approach was applied to **TUN** (which has a doubled *a*-axis) and **IMF** (which has a tripled *b*-axis). The unit cell parameters, space groups and channel sizes and dimensions for the ten framework structures are summarized in Table 1. The unit cell and space group of the idealized SiO_2 framework were used in each case. We found that these unit cell parameters do not deviate significantly from those of the type materials. In this paper, the unit cell dimensions referred to are always those listed in Table 1, rather than those in the literature.

Comparison of the unit cell dimensions and channel direction

The single butterfly layer was extracted from each of the ten frameworks, as shown in Figure 2. It can be seen that all the layers are very similar, apart from some minor geometric distortions. They all have orthogonal axes except for **TUN**, where the angle between *a* and *b* is 93°. The framework structures of the butterfly family are built by stacking the butterfly layers along the *c*-axis, with the layers related to one another by a mirror plane or an inversion center. All the TO_4 tetrahedra in the layer are three-connected, leaving the 4th connection pointing either up (U) or down (D). As indicated in Figure 2, the U and D arrangements of the TO_4 tetrahedra within the butterfly layer differ from structure to structure. Therefore the connections to the neighboring

layers also differ and result in different three-dimensional frameworks.

As shown in Table 1, of the ten frameworks of the butterfly family of zeolites, the building layer in *MRE has the largest unit cell dimensions ($a = 14.562$ Å, $b = 20.314$ Å), so these are used as the reference. The deviations of the *a*- and *b*-parameters from those of *MRE are calculated for each member in the butterfly family, as listed in Table 1. Figure 3 shows the butterfly layers for all the members viewed on the same scale along the *a*- and *b*-axes, respectively, and the differences in the unit cell dimensions are clearly seen. The three-dimensional frameworks of all ten members viewed perpendicular to the *c*-axis are shown in Figure 4, where the connectivities between the layers can be seen.

The *a*-dimension of the **BOG** framework is shorter than that of the *MRE framework by 1.893 Å. This difference can be seen clearly in Figure 3A, where the building layers of *MRE and **BOG** are viewed along the *b*-axis. The layer in *MRE is flat, so the stacking of this layer along the *c*-axis results in close packing (Figure 4). Therefore there are no channels along the *b*-axis. The layer in **BOG**, on the other hand, has significant ripples. This layer is connected to another layer stacked along the *c*-axis, with ripples in the opposite direction. 12-ring channels along the *b*-axis are therefore created in the ripples, as shown in Figure 4. A comparison of the layers in *MRE and **BOG** shows that there is a direct link between the shortened dimension (along the *a*-axis) and the existence of large channels
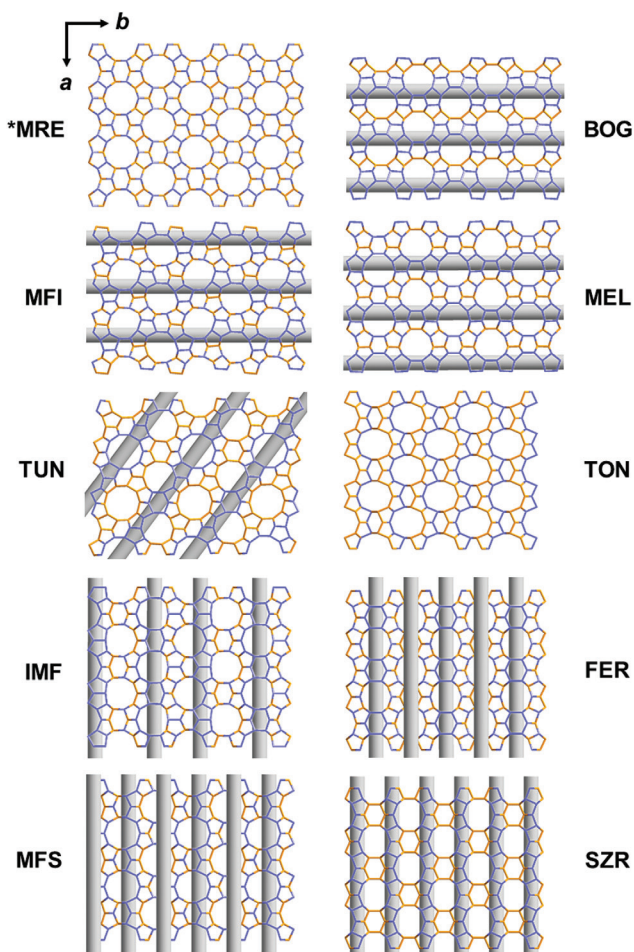
Fig. 2: The butterfly layers extracted from the ten members of the butterfly family viewed perpendicular to the layer. The gray stripes indicate the channels formed as a result of the corrugation of the layers. Only the T–T connections (T = Si, Al) are shown for clarity. The T atoms pointing up are in blue and those pointing down are in gold.

Fig. 3: Projections of the butterfly layers for the members of the butterfly family along (A) the *b*-axis and (B) the *a*-axis. The gray spheres indicate the projections of the channels formed as a result of the corrugation of the layers. Only the T–T connections (T = Si, Al) are shown for clarity. The T-atoms pointing up are in blue and those pointing down are in gold. For comparison, the layers are shown on the same absolute scale.

along the direction perpendicular to the shortened dimension (along the *b*-axis). This can be understood easily from the fact that the T–O distances in zeolite framework structures are very well defined. The shortening along a dimension of the butterfly layer inevitably creates ripples along the same direction, which in turn creates channels in the direction perpendicular to it.

The *b*-dimension of **BOG** is shorter than that of *MRE by 0.300 Å. The difference in this dimension is much smaller than that along the *a*-axis. It can be seen that both the layers are flat along the *b*-axis (Figure 3B). The stacking of these flat layers along the *c*-axis results in close packing and channels are absent along the *a*-axis. Following the analysis for the *b*-dimensions of *MRE and **BOG** above, we can conclude that if a unit cell dimension of the butterfly layer shows little difference from the corresponding dimension in *MRE, the layer can be expected to be
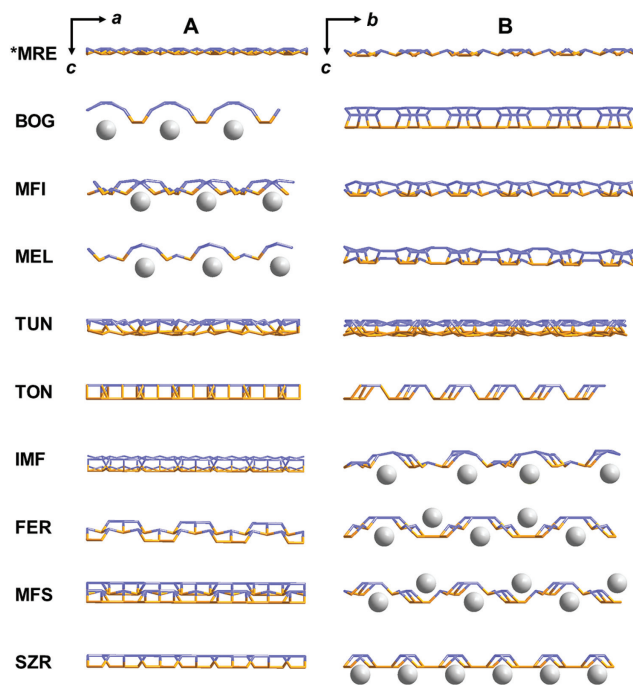
flat along that direction and no channels will form along the perpendicular direction.

The analysis above can be applied to the observations for framework structures **MEL** and **MFI** also. They show changes in the *a* and *b* unit cell dimensions similar to those of **BOG**. **MEL** has *a*-and *b*-dimensions shorter than those of *MRE by 1.103 Å and 0.044 Å, respectively, while for **MFI** the differences are 1.420 Å and 0.224 Å, respectively. Both frameworks have 10-ring channels along the *b*-axis (Figures 3 and 4). The shortening of the *b*-axis is small for both **MEL** and **MFI**, similar to that in **BOG**. Accordingly, no channels are expected along the *a*-axis.

In contrast to **BOG**, **MEL** and **MFI**, the *a*-dimensions of the frameworks **SZR**, **MFS**, **FER** and **IMF** are only slightly shorter than that of *MRE, with the differences ranging from 0.161 Å to 0.266 Å. As expected from the above analysis and also seen in Figure 3, no channels are present along the *b*-axes. For these four framework structures, the shortening of the *b*-axes is larger, ranging from 1.296 Å to 1.385 Å. This is comparable to the shortening of the *a*-axes for **BOG**, **MEL** and **MFI**. Therefore we expect **SZR**, **MFS**, **FER** and **IMF** to have channels running parallel to the *b*-axes. Indeed, **SZR**, **MFS** and **FER** have 8-ring

channels along the *b*-axes, while **IMF** has 10-ring channels along the same direction.

The framework structures described above display a significant shortening along either the *a*- or the *b*-axis, with only small changes in the other. **TUN**, however, shrinks along both the *a*- and the *b*-axes, by 0.640 Å and 0.717 Å, respectively. These differences are about half those observed for the frameworks with a shrinkage along a single axis. There are no channels along either the *a*-axis or *b*-axis in **TUN** (Figure 3). However, if we consider the diagonal of the unit cell, it has shrunk by 0.989 Å, which is then comparable to the shrinkage observed in the previously described structures. Indeed, **TUN** has 10-ring channels running along the diagonal (Figures 2 and 4).

The *a*-axis of the **TON** framework is shorter than that of *****MRE** by 0.457 Å. This is larger than the shortening of the *a*-axes of **SZR**, **MFS**, **FER** and **IMF** which do not have channels along the *b*-axis, but smaller than **TUN** which has channels along the diagonal. This would suggest that the **TON** framework has no channels along the *b*-axis or the diagonal. The *b*-axis of the **TON** framework is shorter than that of *****MRE** by 2.472 Å. This is the largest deviation seen for any of the members of the butterfly family. By looking at this large deviation alone, we would expect large channels along the *a*-axis. However, **TON** has a very short unit cell (5.256 Å) along the stacking direction (*c*-axis), which precludes the presence of any channels (Figure 3). The **TON** framework has only one-dimensional 10-ring channels along the *c*-axis. Although the **TON** framework has the shortest *b*-axis of all the members of the butterfly family, there are no large ripples in the butterfly net (Figure 3).

Prediction of the ring sizes and channel dimensions

The analysis above shows that the shrinking of the unit cells of the butterfly layer relative to that of the *****MRE** framework can be used to deduce the presence and directions of channels perpendicular to the stacking direction of the layers. There seems to be a correlation between the *c*-parameter and the ring sizes of the channels. **BOG**, with the longest *c*-axis (23.6 Å), has 12-ring channels (and the largest shrinkage along the *a*-axis), while those with 20 Å *c*-axes (**MFI**, **MEL**, **TUN**, and **IMF**) have 10-ring channels, those with 7.5 Å *c*-axes (**FER**, **MFS** and **SZR**) have 8-ring channels, and **TON**, with a 5.3 Å *c*-axis has no channels. However, it must be noted that the reference structure *****MRE**, with a *c*-axis of 8.3 Å and no channels does not fit

into this scheme. We also noticed that in each of the ten zeolite frameworks of the butterfly family, a mirror plane perpendicular to the *c*-axis is always present. It is interesting to study in detail how the channel size and dimension are related to the *c*-parameter and the symmetry. The full channel systems of the ten zeolite members in the butterfly family are shown in Figure 5.

Although the **TON** framework has the largest shrinkage of the *b*-axis of all the members of the butterfly family, there is no channel parallel to the butterfly layer because the *c*-axis (5.256 Å) is too short. **TON** has the space group *Cmcm*, so all the T-atoms have to lie on the mirror plane perpendicular to the *c*-axis to avoid short T···T distances (Figure 4).
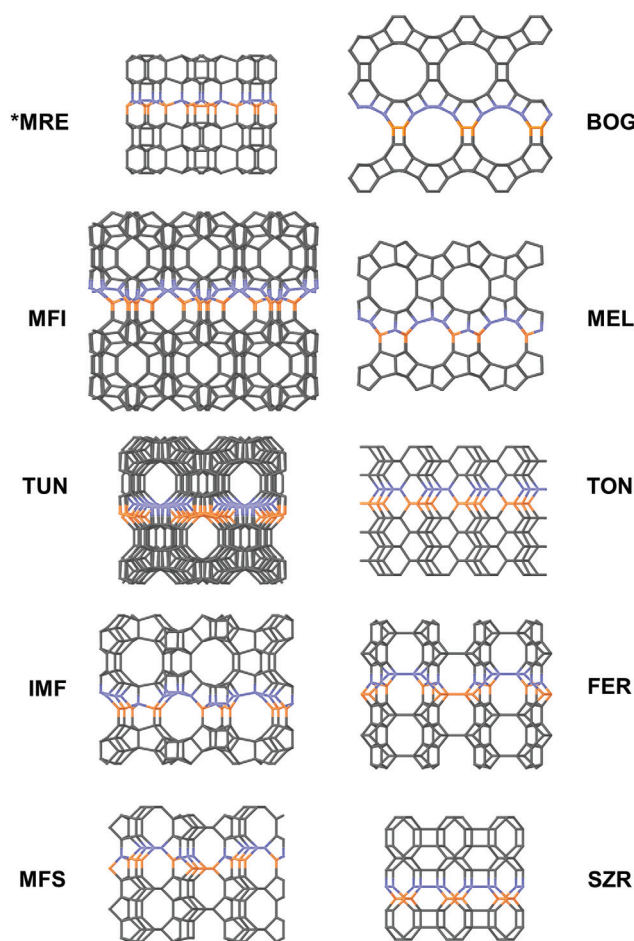

Fig. 4: The 3D framework structures of the ten butterfly family of zeolites viewed along the *a*-axis for *****MRE**, **TON**, **IMF**, **FER**, **MFS** and **SZR**, along the *b*-axis for **BOG**, **MFI** and **MEL**, and along [101] for **TUN**. The *c*-axis is vertical for all structures. Only the T–T connections (T = Si, Al) are shown for clarity. One butterfly layer is highligted in each structure, with the T-atoms pointing up in blue and those pointing down in gold.

The next group, **FER**, **MFS** and **SZR**, have c-axes close to 7.5 Å. A search in the Database of Zeolite Structures shows that no zeolite with a cell dimension of <8 Å has 10- or larger ring channels perpendicular to that direction. The space group is $Immm$ for **FER**, $Im2m$ for **MFS**, and $Cmmm$ for **SZR**. In all three, half of the symmetry-independent T-atoms lie on the mirror plane perpendicular to the c-axis (Figures 3 and 4). The mirror generates a double layer of butterfly layers that share the T-atoms on the mirror plane. The double layers are further connected along the c-axis to form a 3D framework. A c-axis of 7.5 Å only allows one such double layer per unit cell and the channels are also on the mirror planes. Thus the channel is most likely to have an 8-ring pore opening. In **FER** and **MFS**, the 8-ring channels are arranged in a centered manner in the ac projection following the body-centering (Figure 4), while in **SZR**, the 8-ring channels are arranged in an orthogonal manner (Figures 3 and 4). In **SZR**, the 10-ring channels along the c-axis are between the 8-ring channels along the a-axis (Figure 2), resulting in the short distance of $1/4b$ (4.72 Å) between the centers of the 8- and 10-ring channels. This short distance means that each 10-ring channel connects to the two 8-ring channels on either side of it to form a 3D channel system (Figure 5). All the channels are inter-connected. In **FER** and **MFS**, the 10-ring channels along the c-axis intersect the 8-ring channels along the a-axis exactly (Figure 2) and are far away from other 8-ring channels, resulting in 2D channel systems (Figure 5).

It is interesting to understand why ***MRE** does not have any channels perpendicular to the c-axis, although it has a large c-dimension (8.257 Å). One possible reason could be that the increase in the c-axis compared to those for **FER**, **MFS** and **SZR** makes it difficult to place any T-atoms on the mirror plane. The butterfly layers in ***MRE** do not share any common T-atoms as they do in **FER**, **MFS** and **SZR**. ***MRE** has the space group $Imcm$. The c-axis of 8.257 Å only allows two butterfly layers per unit cell. The mirror plane has to be located half-way between the layers to avoid short T···T distances, so all the T···T connections between the layers are perpendicular to the layer. The flat butterfly layer combined with the T···T connections between the layers precludes the formation of channels perpendicular to the c-axis.

The **MFI**, **MEL**, **TUN** and **IMF** frameworks have similar c parameters of about 20 Å, with the space groups $Pbnm$, $I\bar{4}m2$, $B112/m$, and $Cmcm$, respectively. All four have double butterfly layers. These double layers are different for different structures, because of the different UD arrangements in the butterfly layers. However, each has two double layers per unit cell, located half-way between the mirror planes perpendicular to the c-axis. They all
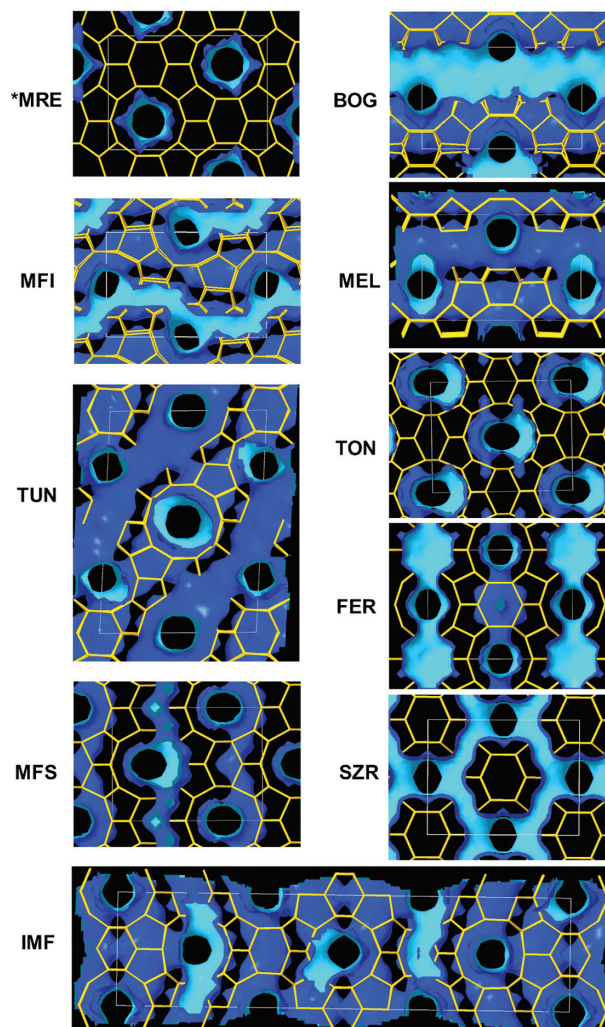

Fig. 5: The channel systems in the frameworks of the butterfly family. The inner and outer surfaces of the channels are shown in cyan and blue, respectively.

have 10-ring channels perpendicular to the c-axis, located on the mirror planes. The channels are arranged in a centered manner, generated by the n-glide plane perpendicular to the b-axis for **MFI**, by the I-centering for **MEL**, and by the B-centering for **TUN**. The 10-ring channels along the c-axis connect with the 10-ring channels perpendicular to them, but at different heights, so 3D channel systems are formed (Figure 5). All channels in **MFI**, **MEL** and **TUN** are inter-connected. In **IMF**, the 10-ring channels are not equally spaced along the long b-axis (56 Å) (Figure 2). As a result, the 10-ring channels along the c-axis only connect with some of the 10-ring channels perpendicular to them, but at different heights. Thus, the channel system is 3D locally, but there are walls between these 3D sections making the channel system 2D.

The last member, **BOG**, has the longest c-axis (23.58 Å) with the space group $Imcm$. As in the previous group, two

butterfly layers form a double layer and there are two double layers per unit cell. These are located half-way between the mirror planes perpendicular to the *c*-axis. There are 12-ring channels perpendicular to the *c*-axis, located on the mirror planes. The channels are arranged in a centered manner, generated by the *I*-centering. The 10-ring channels along the *c*-axis intersect the 12-ring channels perpendicular to them, but at different heights to form a 3D channel system (Figure 5).

We have shown that it is possible to deduce the size of the pore opening and the channel dimension based on the unit cell dimensions and symmetry. However, it is difficult to determine the position of the channels with respect to the layers. It can be seem from Figure 2 that the channels along the same directions (along the *a*- or *b*-axes) appear at different positions relative to the layers in different structures.

Other structures related to the butterfly family

The ten members of the butterfly family found in the database can all be built simply by stacking the butterfly layer along its normal. All the layers are related by symmetry (mirror planes or inversion centers). Another nine framework structures in the database (**PCR, -SVR, OKO, SFS, CON, TER, MEP, MTN,** and **GON**) also contain butterfly layers, but they cannot be constructed from these layers alone (Figure 6).

The **MTT** framework has unit cell dimensions $a = 5.256$ Å, $b = 22.031$ Å, $c = 11.384$ Å and space group *Pmmn*. A layer perpendicular to the *a*-axis is cut out from the **MTT** framework and shown in Figure 6a. **MTT** is built by stacking this layer along the *a*-axis. It can be seen that the layer is similar to that of the butterfly family, but it is not identical (the "butterflies" are arranged differently).

The **PCR** framework has unit cell dimensions $a = 20.1437$ Å, $b = 14.0723$ Å, $c = 12.5223$ Å and space group *C2/m*. A butterfly layer in the *ab* plane of the **PCR** framework is shown in Figure 6b. The unit cell dimensions of this layer are very similar to those of the layers in the butterfly family. However, the **PCR** framework cannot be built from this layer and its symmetry related ones alone. In the [010] projection of **PCR** (Figure 6c), it can be seen that **PCR** requires additional building units and that the stacking is not along the normal to the layers, resulting in a β angle very different from 90°. The remaining eight zeolites framework types shown in Figure 6c also require additional building units to complete the structure.
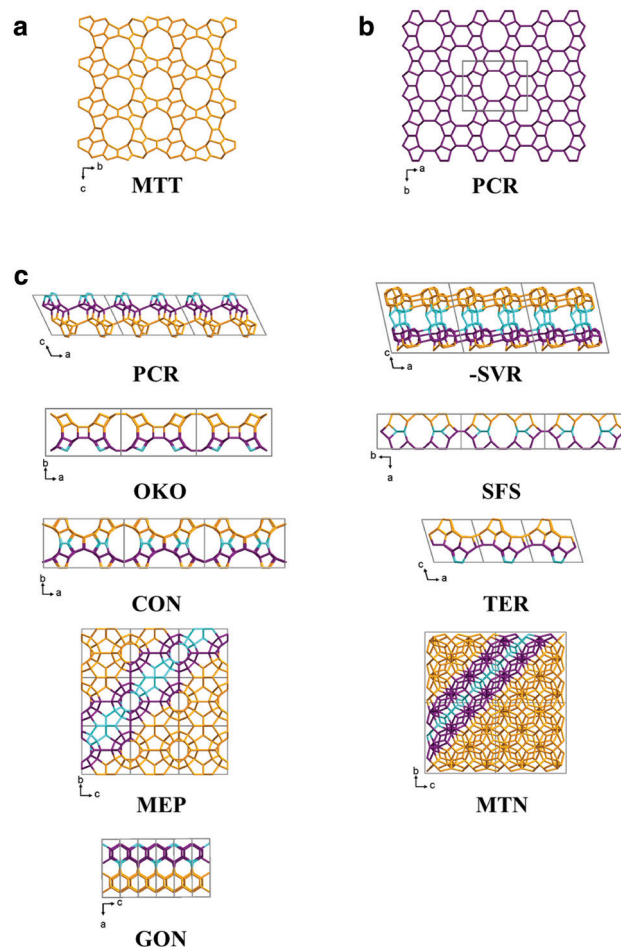

Fig. 6: (a) The layer in **MTT** (with a different arrangement of "butterflies") viewed along the *a*-axis. (b) The butterfly layer in **PCR**. (c) Nine frameworks that contain butterfly layers, but cannot be built from them alone. The butterfly layers are marked in dark purple and the extra units needed to construct the structure in cyan.

Conclusions

We have identified ten zeolite frameworks from the Database of Zeolite Structures that can be built only from layers corresponding to a butterfly net containing 5-, 6- and 10-rings. Different orientations of the TO_4 tetrahedra with respect to the layer and the resulting connectivity to neighboring butterfly layers result in a variety of zeolite frameworks with different channel systems. We found that the direction of the channels parallel to the layer affect the unit cell parameters of the layer. By taking the length of the *c*-axis and the symmetry into account, it may also be possible to predict the size and dimensionality of the channels. This may be helpful for prediction of new members in the butterfly zeolite family.

References

[1] C. Baerlocher, L. B. McCusker, Database of zeolite structures. http://www.iza-structure.org/databases/. The 3-letter codes assigned to the unique framework types in this database are given for each material in boldface text throughout the manuscript.

[2] W. Baur, On cation + water positions in faujasite. *Am. Mineral.* **1964**, *49*, 697.

[3] G. T. Kokotailo, S. L. Lawton, D. H. Olson, W. M. Meier, Structure of synthetic zeolite ZSM-5. *Nature* **1978**, *272*, 437.

[4] W. M. Meier, The crystal structure of mordenite (ptilolite)*. *Z. Kristallogr.* **1961**, *115*, 439.

[5] P. A. Vaughan, The crystal structure of the zeolite ferrierite. *Acta Crystallogr.* **1966**, *21*, 983.

[6] J. M. Newsam, M. M. J. Treacy, W. T. Koetsier, C. B. D. Gruyter, Structural characterization of zeolite beta. *Proc. R Soc. Lond. Math. Phys. Sci.* **1988**, *420*, 375.

[7] R. Barrer, H. Villiger, Crystal structure of synthetic zeolite L. *Z. Kristallogr.* **1969**, *128*, 352.

[8] R. Pophale, P. A. Cheeseman, M. W. Deem, A database of new zeolite-like materials. *Phys. Chem. Chem. Phys.* **2011**, *13*, 12407.

[9] M. M. J. Treacy, K. H. Randall, S. Rao, J. A. Perry, D. J. Chadi, Enumeration of periodic tetrahedral frameworks. *Z. Kristallogr.* **1997**, *212*, 768.

[10] Y. Li, J. Yu, New stories of zeolite structures: their descriptions, determinations, predictions, and evaluations. *Chem. Rev.* **2014**, *114*, 7268.

[11] M. W. Deem, R. Pophale, P. A. Cheeseman, D. J. Earl, Computational discovery of new zeolite-like materials. *J. Phys. Chem. C* **2009**, *113*, 21353.

[12] M. D. Foster, M. M. J. Treacy, Progress towards an atlas of designer zeolites. In Stud. Surf. Sci. Catal., (Eds. R. Xu, Z. Gao J. Chen and W. Yan) Elsevier, Amsterdam. **2007**, p. 666.

[13] A. Le Bail, Predicted Crystallography Open Database.

[14] H. Gies, H. van Koningsveld, Catalog of disorder in zeolite frameworks. http://www.iza-structure.org/databases/.

[15] F. Hawthorne, J. Smith, Enumeration of 4-connected 3-dimensional nets and classification of framework silicates combination of zigzag and saw chains with 6^3, 3.12^2, 4.8^2, $4.6.12$ and $(5^2.8)_2(5.8^2)_1$ Nets. *Z. Kristallogr.* **1988**, *183*, 213.

[16] L. B. McCusker, C. Baerlocher, Chapter 2 Zeolite structures. In Stud. Surf. Sci. Catal., (Eds. J. Čejka, H. van B., A. Corma and F. Schüth) Elsevier, Amsterdam. **2007**, p. 13.

[17] J. B. Higgins, R. B. LaPierre, J. L. Schlenker, A. C. Rohrman, J. D. Wood, G. T. Kerr, W. J. Rohrbaugh, The framework topology of zeolite beta. Zeolites. **1988**, *8*, 446.

[18] A. W. Burton, S. Elomari, I. Chan, A. Pradhan, C. Kibby, Structure and synthesis of SSZ-63: toward an ordered form of Zeolite beta. *J. Phys. Chem. B* **2005**, *109*, 20266.

[19] Z. B. Yu, Y. Han, L. Zhao, S. L. Huang, Q. Y. Zheng, S. Z. Lin, A. Cordova, X. D. Zou, J. L. Sun, Intergrown new zeolite beta polymorphs with interconnected 12-ring channels solved by combining electron crystallography and single-crystal x-ray diffraction. *Chem. Mater.* **2012**, *24*, 3701.

[20] L. Q. Tang, L. Shi, C. Bonneau, J. L. Sun, H. J. Yue, A. Ojuva, B. L. Lee, M. Kritikos, R. G. Bell, Z. Bacsik, et al. A zeolite family with chiral and achiral structures built from the same building layer. *Nat. Mater.* **2008**, *7*, 381.

[21] A. W. Burton, Structure solution of zeolites from powder diffraction data. *Z. Kristallogr.* **2009**, *219*, 866.

[22] The most common composite building units have been assigned codes by the IZA-SC and are listed in the Database of Zeolite Structures.

[23] D. Xie, L. B. McCusker, C. Baerlocher, S. I. Zones, W. Wan, X. D. Zou, SSZ-52, a Zeolite with an 18-layer aluminosilicate framework structure related to that of the DeNOx catalyst Cu-SSZ-13. *J. Am. Chem. Soc.* **2013**, *135*, 10519.

[24] M. Moliner, T. Willhammar, W. Wan, J. Gonzalez, F. Rey, J. L. Jorda, X. D. Zou, A. Corma, Synthesis design and structure of a multipore zeolite with interconnected 12-and 10-MR channels. *J. Am. Chem.* Soc. **2012**, *134*, 6473.

[25] D. Akporiaye, Structural relationships of zeolite frameworks – 5-ring zeolites. *Z. Kristallogr.* **1989**, *188*, 103.

[26] J. L. Schlenker, W. J. Rohrbaugh, P. Chu, E. W. Valyocsik, G. T. Kokotailo, The framework topology of ZSM-48: A high silica zeolite. *Zeolites* **1985**, *5*, 355.

[27] C. A. Fyfe, H. Gies, G. T. Kokotailo, C. Pasztor, H. Strobl, D. E. Cox, Detailed investigation of the lattice structure of zeolite ZSM-11 by a combination of solid-state NMR and synchrotron x-ray diffraction techniques. *J. Am. Chem. Soc.* **1989**, *111*, 2470.

[28] K. G. Strohmeier, M. Afeworki, D. L. Dorset, The crystal structures of polymorphic SUZ-4. *Z. Kristallogr.* **2009**, *221*, 689.

[29] J. L. Schlenker, J. B. Higgins, E. W. Valyocsik, The framework topology of ZSM-57: a new synthetic zeolite. *Zeolites* **1990**, *10*, 293.

[30] F. Gramm, C. Baerlocher, L. B. McCusker, S. J. Warrender, P. A. Wright, B. Han, S. B. Hong, Z. Liu, T. Ohsuna, O. Terasaki, Complex zeolite structure solved by combining powder diffraction and electron microscopy. *Nature* **2006**, *444*, 79.

[31] C. Baerlocher, F. Gramm, L. Massuger, L. B. McCusker, Z. B. He, S. Hovmoller, X. D. Zou, Structure of the polycrystalline zeolite catalyst IM-5 solved by enhanced charge flipping. *Science* **2007**, *315*, 1113.

[32] J. Pluth, J. Smith, Crystal-structure of boggsite, a new high-silica zeolite with the 1st 3-dimensional channel system bounded by both 12-rings and 10-rings. *Am. Mineral.* **1990**, *75*, 501.

[33] S. A. I. Barri, G. W. Smith, D. White, D. Young, Structure of theta-1, the first unidimensional medium-pore high-silica zeolite. *Nature* **1984**, *312*, 533.

[34] B. Marler, C. Deroche, H. Gies, C. A. Fyfe, H. Grondey, G. T. Kokotailo, Y. Feng, S. Ernst, J. Weitkamp, D. E. Cox, The structure of zeolite ZSM-23 (MTT) refined from synchrotron X-ray powder data. *J. Appl. Crystallogr.* **1993**, *26*, 636.

[35] W. J. Roth, P. Nachtigall, R. E. Morris, P. S. Wheatley, V. R. Seymour, S. E. Ashbrook, P. Chlubná, L. Grajciar, M. Položij, A. Zukal, et al. A family of zeolites with controlled pore size prepared using a top-down method. *Nat. Chem.* **2013**, *5*, 628.

[36] Ch. Baerlocher, D. Xie, L.B. McCusker, S.-J. Hwang, I. Y. Chan, K. Ong, A. W. Burton, S. I. Zones, Ordered silicon vacancies in the framework structure of the zeolite catalyst SSZ-74. *Nat. Mater.* **2008**, *7*, 631.

[37] E. Verheyen, L. Joos, K. Van Havebergh, E. Breynaert, N. Kasian, E. Gobechiya, K. Houthoofd, C. Martineau, M. Hinterstein, F. Taulelle, V. Van Speybroeck, M. Waroquier, S. Bals, G. Van Tendeloo, Inverse sigma transofrmation. *Nat. Mater.* **2012**, *11*, 1059.

[38] S. Elomari, A. Burton, R. C. Medrud, R. Grosse-Kunstleve, The synthesis, characterization, and structure solution of SSZ-56: An extreme example of isomer specificity in the structure direction of zeolites. *Microporous Mesoporous Mat.* **2009**, *118*, 325.

[39] R.F. Lobo, M. E. Davis, CIT-1: a new molecular sieve with intersecting pores bounded by 10- and 12-rings. *J. Am. Chem. Soc.* **1995**, *117*, 3766.

[40] E. Galli, S. Quartieri, G. Vezzalini, A. Alberti, M. Franzini, Terranovaite from antarctica: a new 'pentasil' zeolite. *Am. Mineral.* **1997**, *82*, 423.

[41] H. Gies, Studies on clathrasils. III. Crystal structure of melanophlogite, a natural clathrate compound of silica. *Z. Kristallogr.* **1983**, *164*, 247.

[42] J. L. Schlenker, F. G. Dwyer, E. E. Jenkins, W. J. Rohrbaugh, G. T. Kokotailo, W. M. Meier, Crystal structure of a synthetic high silica zeolite – ZSM-39. *Nature* **1981**, *294*, 340.

[43] J. Plévert, Y. Kubota, T. Honda, T. Okubo, Y. Sugi, GUS-1: a mordenite-like molecular sieve with the 12-ring channel of ZSM-12. *Chem. Commun.* **2000**, 2363.

[44] V. A. Blatov, *Struct. Chem.* **2012**, *23*, 955. (http://topospro.com).